

# Experimental studies into a new type of hybrid outrigger system with metal dampers

A.J. Wang\*

Centre of Innovation for Building and Construction, CapitalLand China Corporate, Shanghai, P.R. China

(Received February 7, 2017, Revised June 16, 2017, Accepted June 19, 2017)

**Abstract.** This paper presents the experimental investigation into a new type of steel-concrete hybrid outrigger system developed for the high-rise building structure. The steel truss is embedded into the reinforced concrete outrigger wall, and both the steel truss and concrete outrigger wall work compositely to enhance the overall structural performance of the tower structures under extreme loads. Meanwhile, metal dampers of low-yield steel material were also adopted as a 'fuse' device between the hybrid outrigger and the column. The damper is engineered to be 'scarified' and yielded first under moderate to severe earthquakes in order to protect the structural integrity of important structural components of the hybrid outrigger system. As such, not brittle failure is likely to happen due to the severe cracking in the concrete outrigger wall. A comprehensive experimental research program was conducted into the structural performance of this new type of hybrid outrigger system. Studies on both the key component and overall system tests were conducted, which reveal the detailed structural response under various levels of applied static and cyclic loads. It was demonstrated that both the steel bracing and concrete outrigger wall are able to work compositely with the low-yield steel damper and exhibits both good load carrying capacities and energy dispersing performance through the test program. It has the potential to be applied and enhance the overall structural performance of the high-rise structures over 300 m under extreme levels of loads.

**Keywords:** composite structures; physical test; outrigger; damper; high-rise building

## 1. Introduction

A new type of steel-concrete hybrid outrigger system is developed in two mega high-rise towers of 370 m tall in Raffles City Chongqing (Wang 2015), in which the steel truss is innovatively embedded into the reinforced concrete outrigger wall as shown in Fig. 1(a) and 1(b). Both the steel truss and concrete outrigger wall works compositely to enhance the overall structural performance of the tower structures under extreme loads. Meanwhile, metal dampers of low-yield steel material were also adopted as a 'fuse' device between the hybrid outrigger and the mega column. The dampers are engineered to be 'scarified' and yielded first under moderate to severe earthquakes in order to protect the structural integrity of important structural components of the hybrid outrigger system. As such, not brittle failure is likely to happen due to the severe concrete cracking. This hybrid system leads to a higher level of structural integrity and energy dispersing performance as compared with other conventional steel outrigger system. Another advantage is that the design may allow the contractor to break through the critical path of the tedious welding on the steel outrigger truss in the refugee floors, and 'shoot' the core by leaving the construction joints between the core and the outrigger walls, which contributes to shortening the overall construction period of the high rise

structure as well.

This paper presents the experimental investigation into the structural performance of this new type of hybrid outrigger system. Both the key component and overall system tests were conducted, which reveal the detailed structural response under various levels of monotonic and quasi-static cyclic loads. The metal dampers are verified to be able to work effectively under earthquakes and enhance the overall structural performance. It is also demonstrated that the hybrid outrigger system exhibits sufficient ductility under the seismic action with the effective protection for the 'fuse' device of the low-yield steel damper.

## 2. Literature review and scope of work

### 2.1 Steel and composite outrigger

The effectiveness of outrigger system on the modern highrise building was investigated since 1980s. Smith and Irawan (1981) established analytical approach to assess the deflection and internal forces in both the moment frame and the braced moment frame structures with the steel outrigger. The analytical results were calibrated through both virtual energy approach and minimum potential energy approach. Design formulae were derived for the calculation of the distribution inter-floor drifting and internal forces and moments on typically rectangular shape buildings. These design formulae was further adopted by Smith and Irawan (1983), Coull and Lao (1988) to establish the optimum structural layout for typical high-rise buildings with

---

\*Corresponding author, Ph.D.  
E-mail: [aaron.juan.wang@icloud.com](mailto:aaron.juan.wang@icloud.com)

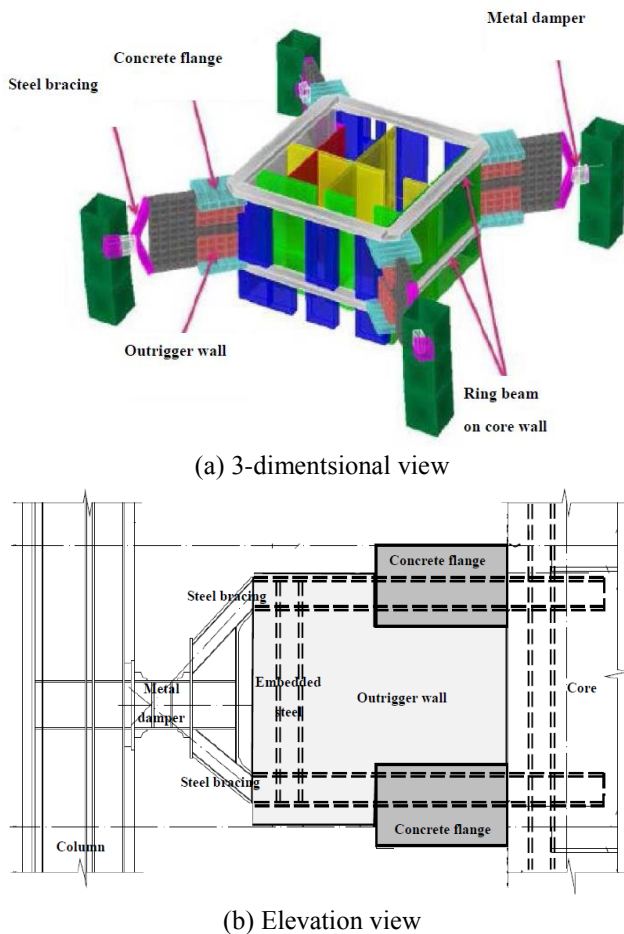


Fig. 1 Hybrid outrigger system

outriggers and under earthquakes. The analytical investigation on the free vibration mode was also conducted by Moudarre and Coull in 1985. Various components of the steel and composite outrigger and connection system were also studied in the past decade. The coupling effect between the concrete and steel shear wall and the outrigger truss was studied by Lee *et al.* (2008), Gholipour *et al.* (2015) respectively. The effectiveness on the shear wall and the outrigger truss on the foundation settlement were also studied both numerically and analytically by Hoenderkamp in 2004. Lee (2016) studied the utilization rate of steel outrigger system under both two-dimensional and three-dimensional scenarios. Both experimental and numerical investigations were conducted by Nie *et al.* (2014) on the performance of the  $k$ -style joint between the outrigger truss and concrete core.

## 2.2 Numerical investigation and design optimization

With the advances in the finite element technique and numerical optimization technology, more numerical investigation was conducted on buildings with steel outrigger trusses (Wu and Li 2003). More research works on the effectiveness of steel outrigger trusses on concrete core plus moment frame structures were conducted by Bayati *et al.* (2008), Malekinejad and Reza (2011), Zhang *et al.* (2007). Both design formulae and guidance were

established considering the contribution from both the concrete core wall and the steel outrigger truss. Wang (2010) proposes a three dimensional finite element model and a simplified two-dimensional finite element model to study the nonlinear structural behaviour of composite end-plate connections under gravity loads. The three-dimensional finite element model was extended by Wang (2011) to study the structural behaviour of end-plate composite connections under combined gravity and lateral loads. Further research by Moon (2013, 2015) gave more insight and understanding on the performance of high-rise buildings of a larger variety of shapes. The numerical approach was further extended to optimize the structural performance of steel and composite buildings with steel outrigger. Material topology optimization was adopted by Lee *et al.* (2015) to optimize the outrigger layout in high-rise buildings. The studies on the steel outrigger under wind loads were conducted by Sabrina and Tabassum in 2016. A genetic-algorithm-base minimum weight approach was adopted by Park *et al.* (2016), Nouri and Ashtari (2015), which gives the optimal design towards the high-rise building the outrigger of the minimum structural self-weight per the same level of structural performance.

## 2.3 Steel hybrid outrigger and belt truss system

With the recent demand on seismic hazard mitigation of the high-rise building, the application of the viscous damper on the steel outrigger and belt truss system was studied recently by Zhou and Li (2014), Zhou *et al.* (2017) for seismic proof of the building structure. An analytical study was conducted on the similar system by Tan *et al.* in 2015. It was observed that the combination of seismic dampers with steel outrigger arms and belt trusses facilitates structural system of both high stability and ductility. In these studies, the stiffness and damping ratio of the viscous damper was normally carefully chosen to suit the stiffness of the steel outrigger arm, and the damping effect is normally designed to be facilitated after the moderate to severe design earthquakes (Zhou and Li 2014, Zhou *et al.* 2017). Modern numerical and computation technologies were also adopted throughout the structural design and analysis with the incorporation of both geometrical and material non-linearities as well as energy dispersing performance of the viscous damper. While up to now, the majority of the research works was on the steel hybrid outrigger truss as well as its effects towards the structural performance of the high-rise building, while there is very few systematical research conducted on concrete and composite outrigger wall. No comprehensive research works conducted on this new type of concrete-steel hybrid outrigger system with the incorporation of metal dampers considering the seismic action.

## 2.4 Object and scope of work

This paper presents the experimental investigation into the structural performance of this new type of hybrid outrigger system. Both the key component and overall system tests were conducted, which reveal the detailed structural response under various levels of monotonic and



Table 1 Low-yield damper Group DA

Specimen	Section A-A	Web	Flange	Stiffener
DA1: Basic scheme				
DA2: Web height increased from 300 to 350 mm.				
DA3: Additional flange at the middle width of the web.				
DA4: Additional flange added at the middle width of the web; reduced web thickness from 11.7 to 6.7 mm.				
DA5: Increased web thickness from 11.7 to 14.2 mm, no stiffener provided.				

control approach is adopted with the applied displacement of  $\pm\Delta_y/2$ ,  $\pm\Delta_y$ ,  $\pm2\Delta_y$ ,  $\pm3\Delta_y$ ,  $\pm4\Delta_y$ ,  $\pm6\Delta_y$ , where  $\Delta_y$  is the displacement at the first yield of the steel connection. The loading protocol ensures a suitable preloading and sufficient applied displacements to test the overall ductility of the composite connection in the meantime. The test methods and procedures stated in CABR (1997) and ASTM (2011) are also considered.

#### 4. Low-yield steel damper

##### 4.1 Specimen and setup

The general length and width of the specimen are 233.3 mm and 200 mm respectively. In order to study the structural performance of various heights of the low-yield steel damper, the heights of the specimen range from 250 to

Table 2 Low-yield damper Group DB

Specimen	Section A-A	Web	Flange	Stiffener
DB1a and DB1b: Basic scheme				
DB2: Reduced web depth from 300 to 250 mm.				
DB3: Web thickness reduced from 11.7 to 6.7 mm.				
DB4: Web thickness reduced from 11.7 to 6.7 mm; additional flange at the middle width of the web.				



Fig. 3 Test setup on steel damper

350 mm with an approximately scale of 1:6. The double web plates of low-yield steel material were adopted in each of the specimen with a typical thickness of 11.7 mm. The grade of the low-yield steel web is typically taken to be S180. Normal grade steel material of S355 was adopted for

the other components of the metal damper.

The detailed dimensions of the test specimens are shown in Fig. 2 and Tables 1 and 2. A total of two groups, namely Group DA and Group DB, of specimens were tested. The thickness of the flanges was typically 6.7 mm for specimens in Group DA and typically 8.3 for the specimens in Group DB. Various damper height and arrangement of flanges and stiffeners are studied in response to the overall structural performance and modes of failure of the low-yield steel damper.

The physical tests were conducted in the Heavy Structural Laboratory of China Academy of Building Research. All of the test specimens were under quasi-static cyclic load with the loading procedures stated in Section 4. Fig. 3 is the general set up of the test specimen. The overall capacity of the loading frame is up to 2500 kN. An axial load of 430 kN was applied on each of the specimen with an axial-loading-to-capacity ratio of 0.1. The application of horizontal loads is of displacement control per the design load carrying and displacement capacities.

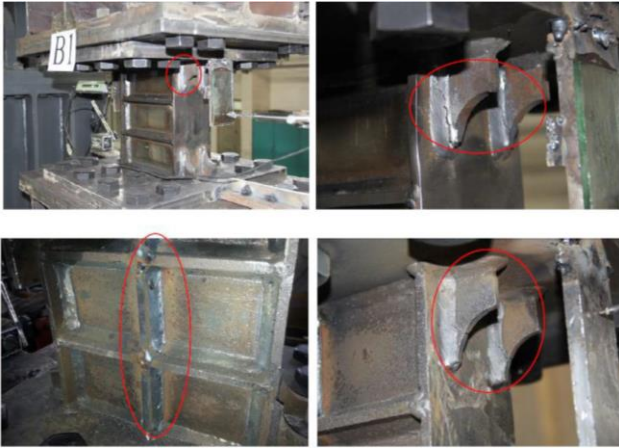


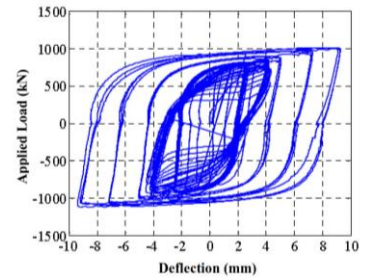
Fig. 4 Specimen after the test

#### 4.2 Test results

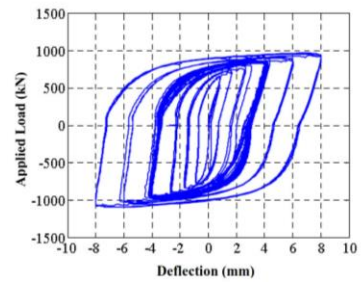
Little degrading in stiffness and strength were observed for the specimen under Group DA under a maximum displacement of  $\pm 2.5$  mm and 30 cycles. While obvious cracks at the joint location among the stiffener, the flange and web were observed under a maximum applied displacement of  $\pm 4$  mm at 15 to 20 cycles. This led to obvious degrading in both stiffness and strength of the specimen. Fig. 4 shows the typical damage mode of the specimen after the tests, while the load-deflection curve of the specimen in Group DA is shown in Fig. 5. The stress concentration is in the vicinity of the stiffeners, which leads to cracks in the welding material and propagated towards to end of the flange. This, in turn, leads to the further damage near the joint location of the flange and the low-yield steel web.

The comparison between the results from Specimens DA1 and DA4 shows that the loading carrying capacity is reduced significantly due to the reduced web thickness in Specimen DA4, which demonstrates the importance of low-yield steel web on the load carrying capacities of the metal damper despite of the additional middle width flange provided in Specimen DA4. Similar findings were observed through the results from Specimen DB1 and DB3 as shown in Fig. 6(a) and 6(d). In Specimen DA5, the low-yield steel web thickness was increased from 11.7 to 14.2 mm as compared with Specimen DA1 shown in Table 1, but result in Fig. 5(e) shows no apparent increase in load carrying capacities. This is because of the omission of the joint stiffener in Specimen DA5 leading to early degrading in both strength and ductility of the damper, which implies the importance of the joint stiffener on the overall strength and ductility of the damper.

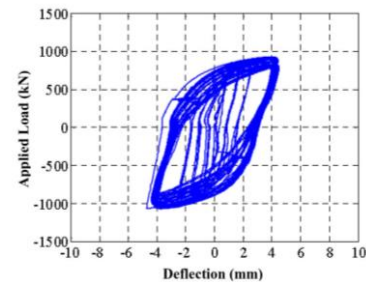
Fig. 6 shows the load-deflection curves for the specimen under Group DB. With the thickened flange from 6.7 to 8.3 mm, the overall performance of the low-yield steel dampers in Group DB is stable under a maximum applied displacement of  $\pm 4$  mm at 30 cycles. Only minor cracks were observed in the joint location between the stiffener and the flange when the maximum applied displacement was up to  $\pm 8$  mm at 30 cycles. No noticeable degrading in damper stiffness and strength was observed. The overall



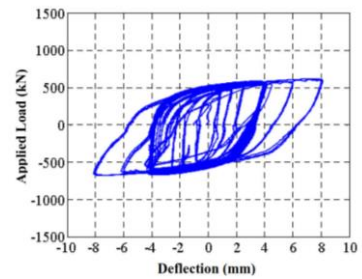
(a) Specimen DA1



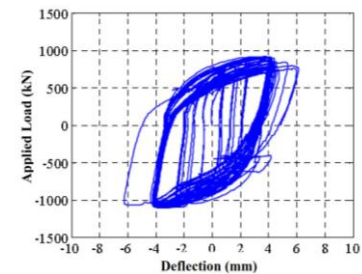
(b) Specimen DA2



(c) Specimen DA3



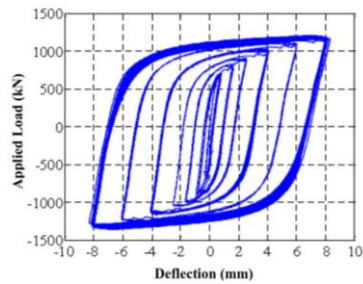
(d) Specimen DA4



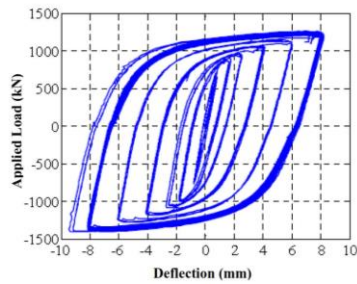
(e) Specimen DA5

Fig. 5 Load deflection curves (Group DA)

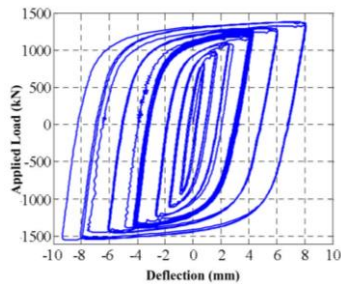
structural integrity of the low-yield steel damper maintained till 60 cycles without major degrading in structural performance. This demonstrates the effectiveness of the thickened damper flange towards the overall ductility and strength of the low-yield steel damper. As such, the



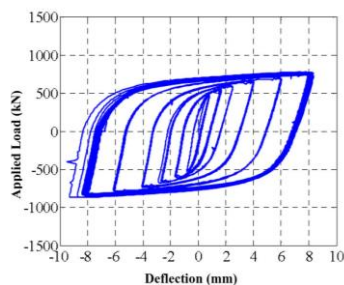
(a) Specimen DB1a



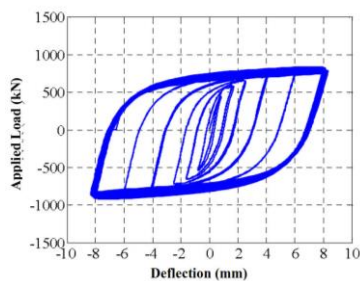
(b) Specimen DB1b



(c) Specimen DB2



(d) Specimen DB3



(e) Specimen DB4

Fig. 6 Load deflection curves (Group DB)

thickness and number of flanges in the low-yield steel damper should be an important consideration in the engineering and detailing of such low-yield steel dampers in the hybrid outrigger system.

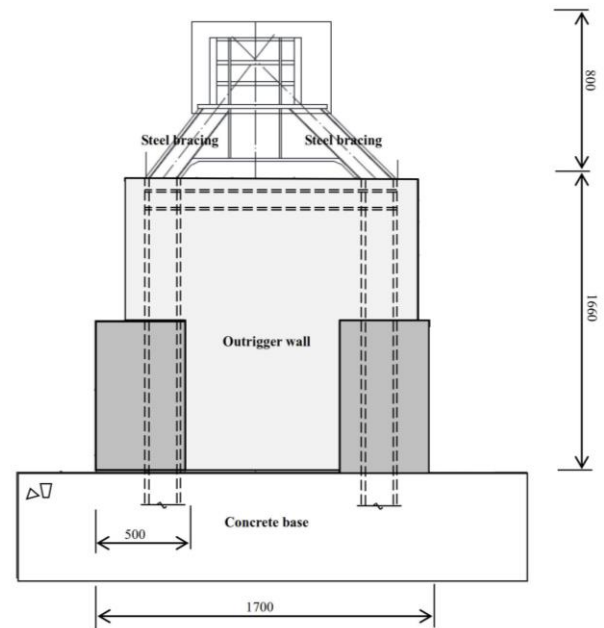


Fig. 7 Details of hybrid outrigger arm

Table 3 Material properties for test groups HOA and HOD

Specimen	Steel bracing (MPa)	Embedded steel section (MPa)	Reinforcement (MPa)	Concrete (MPa)
HOA1	279	372	484	53
HOA2	279	372	485	55
HOD1	283	373	487	55
HOD2	283	373	486	58

## 5. Hybrid outrigger arm

A total of two specimens of the hybrid outrigger arm were fabricated to be tested under monotonic and quasi-static cyclic loads respectively. No low-yield steel damper was covered in this group of tests. Both welding inspection and testing were conducted to ensure a welding quality throughout the joint regions of the specimen. The scale of the specimen designed to be 1:5. Fig. 7 shows the geometrical configuration of the specimen, while the test set-up is shown in Fig. 8. The loading is applied horizontally with a displacement control mechanism. One 250 ton capacity loading cell was positioned on each side of the loading position of the specimen, which allowed both monotonic and quasi-static cyclic loads to be generated. The steel grade of the bracing member was S275, while that for of other steel members were taken to be S355. C50 concrete was adopted for the concrete portion of the hybrid outrigger arm. Table 3 presets the measured material properties of both the concrete and steel materials.

### 5.1 Monotonic loading test

Specimen HOA1 was tested under monotonic loads. Fig. 9 shows the recorded cracks pattern on the concrete outrigger wall, while the load deflection curves of the specimen is shown in Fig. 10. The initial crack in the concrete section was from the end of the concrete T-shape

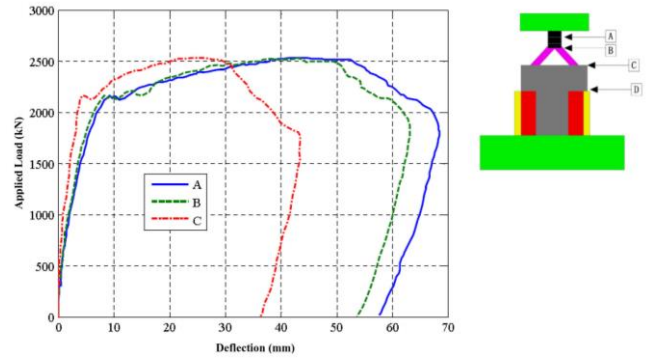
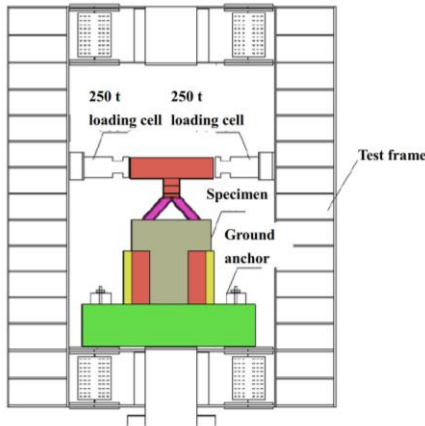


Fig. 10 Load deflection curves for Specimen HOA1

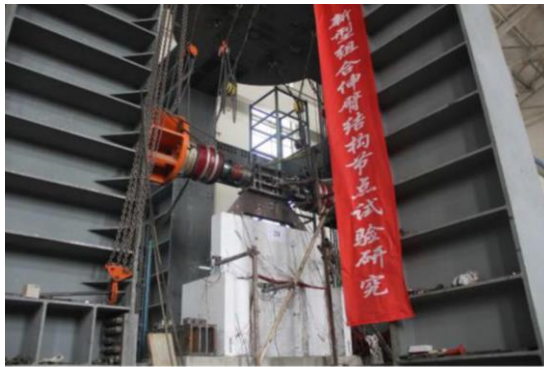
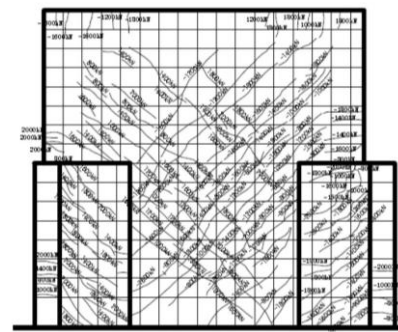
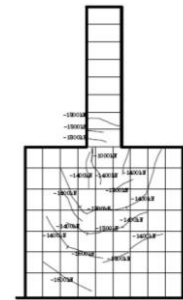


Fig. 8 Test setup for hybrid outrigger arm

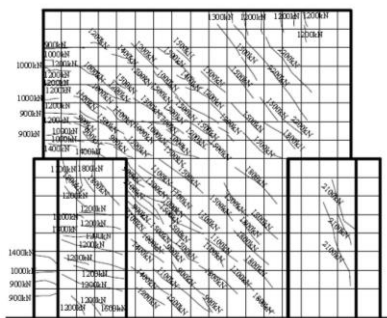


(a) Side view

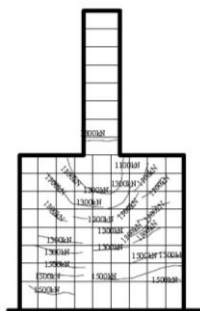


(b) End view

Fig. 11 Cracks on Specimen HOA2



(a) Side view



(b) End view

Fig. 9 Cracks on Specimen HOA1

flanges near the concrete base. Shear cracks were also observed near the upper end portion of the concrete outrigger wall at the load level of 900 kN. This is about 36% of the ultimate load carrying capacities of the outrigger arm with an approximately joint rotation of 1/1100 at the tip

of the steel bracing, and 1/2200 at the tip of the concrete outrigger wall. With the increasing in the applied loads, the cracks further propagated upwards, and the joint between the concrete flange and web of the outrigger wall started cracking. U-shape cracks were observed at the flange section of the concrete outrigger wall with a crack width of approximately 0.05 mm.

The steel bracing started to yield at the load level of 1500 kN per the measurement from the strain gauge along the bracing member, and the crack at the middle concrete section and the joint region between the concrete flange and web continued to grow to approximately 0.1 mm. At the applied load of 2500 kN, the majority of the embedded steel section and the rebar yielded, and the maximum recorded width of the concrete crack reached 0.7 to 1.5 mm, and the unloading was recorded after that as shown in Fig. 10.

### 5.2 Quasi-static cyclic loading test

Specimen HOA2 was tested under quasi-static cyclic

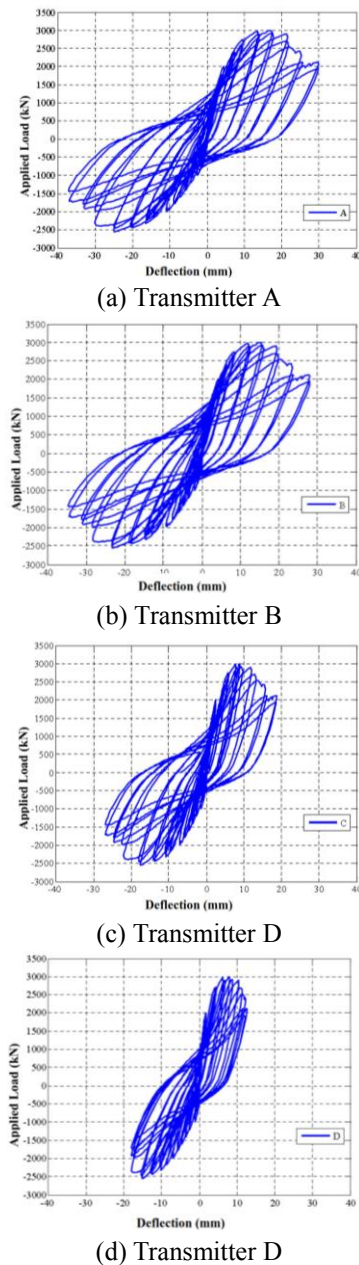


Fig. 12 Load deflection curves for Specimen HOA2

loads. Similar to the monotonic test, the initial cracks in the concrete section happened at the end of the two flanges near the concrete base at the load level of 800 kN. The bi-directional shear cracks were also observed with a crack width of approximately 0.05 mm. This loading level is approximately 30% of the ultimately load carrying capacities of the specimen. The corresponding rotation was 1/1300 at the tip of steel bracing and 1/1700 at the tip of concrete outrigger wall respectively.

Figs. 11 and 12 show the development of concrete cracks and load-deflection characteristics of the specimen. Both the shear crack in the concrete web and the tensile crack in the concrete flange further grown to approximately 0.2 mm at the cyclic load level of 1400 kN. U-shape cracks were also observed on the outer surface of the two concrete flanges of the outrigger wall. Major yielding in steel bracing

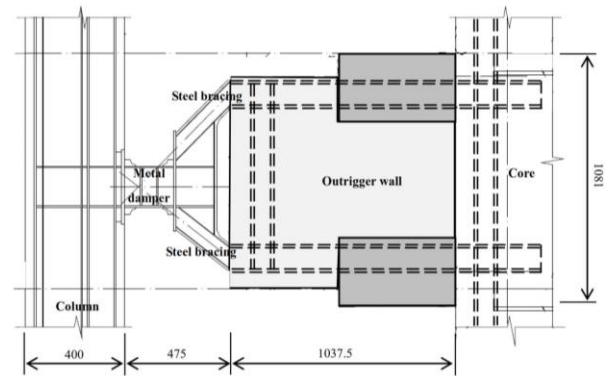


Fig. 13 Details of hybrid outrigger system with damper

and embedded steel sections occurred at the load level of 1800 kN, and the noticeable concrete cracks width was measured to be 0.3 to 1.8 mm. No apparent damage was observed at the 30 cycles of the ultimate load capacity onto the specimen under the maximum deflection of  $\pm 15$  mm, which shown the good composite action and performance of such hybrid outrigger arm. While the degrading in both the strength and the stiffness happened when the maximum applied displacement was larger than 20 mm as shown in Fig. 12. More severe cracks on concrete outrigger wall were also observed through the process. This also implies the necessity of the possible sacrificing member to protect the hybrid outrigger arm from the severe concrete crack and material degrading.

## 6. Hybrid outrigger system with low-yield steel damper

The investigation moved to the system studies by combining the hybrid outrigger arm and the low-yield steel damper. Two system tests were conducted on hybrid outriggers system with low-yield steel dampers under both monotonic and quasi-static cyclic loads. Fig. 13 shows a typical configuration of the test specimen comprising of the concrete core, the hybrid outrigger arm, the low-yield steel dampers and the composite column. For the ease of the specimen erection, only one quarter of the core wall and one hybrid outrigger arm was erected and tested. The scale of the specimens was taken to be 1:8. The steel grade of the bracing members was S275, while that for of other steel members were taken to be S355. C50 concrete was adopted for the concrete portion of the hybrid outrigger arm. Table 3 presents the measured material properties of both the concrete and steel materials. In practice, the belt truss is normally connected and welded to the column, and there is no direct connection between the outrigger system and the belt truss. As such, the current studies focus on the effectiveness of performance of outrigger system, as such, no belt truss is considered in the test program.

S180 low-yield steel dampers were adopted at the connection between the steel bracing member and the composite column. Both the geometrical configuration and material properties of the low-yield steel damper are the same as Specimen DB1 as adopted in the test program for

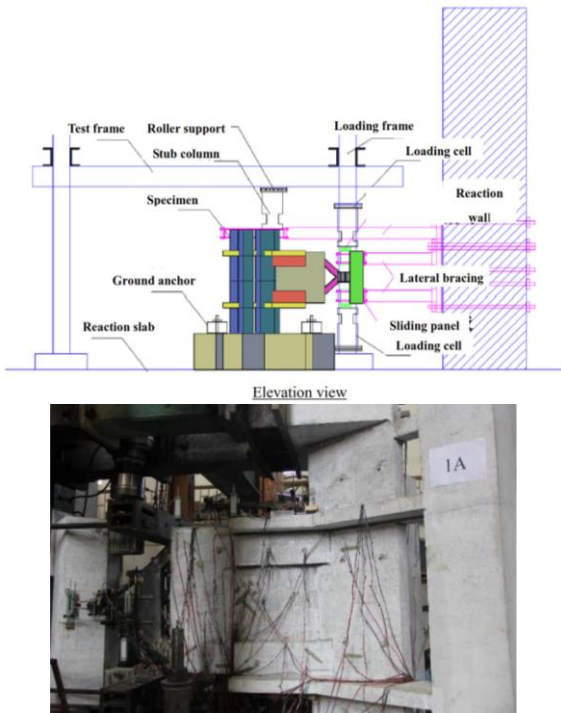


Fig. 14 Test setup for hybrid outrigger system with damper

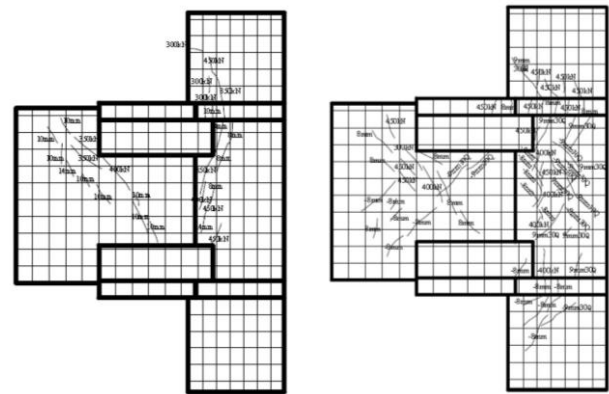
the low-yield steel damper as shown in Table 2. The damper is welded and connected to both the steel bracings and the steel section of the composite column. Fig. 14 shows the overall set up of the test. The loading was applied onto the composite columns as transferred to the hybrid outrigger system through the low-yield steel damper. The detailed findings of the tests are presented in the following paragraphs. A total of two loading cells were adopted, and one was placed on the top and the other was on the bottom side of the column to generate both the monotonic and quasi-static cyclic loads. Bracings were also placed to ensure the stability of the composite column during the test. Sliding panels were placed between the bracing and the column to prevent any possible friction generated through the loading and unloading process.

### 6.1 System test under monotonic loads

Specimen HOD1 was tested under a monotonic loading history. The crack initiated from the concrete ring beam around the core region. The width of the crack is 0.05 mm at a load level of 300 kN. With the increasing in the applied load, very minor cracks also appeared near the *T*-joint between the flange and the web of the concrete outrigger wall. These cracks further grew towards the end of the outrigger wall near the core wall with a maximum crack width of 0.05 mm. The development of the crack in both the outrigger and the core wall is slow with the increase in the load with a maximum width of 0.1 mm at the yielding of the low-yield steel damper as shown in Fig. 15. In the meanwhile, the maximum recorded crack width is approximately 0.15 mm, which happened on the ring beam around the concrete core wall. Fig. 16(a) shows the development of the crack on both the core and the concrete



Fig. 15 Yielding on low-yield steel damper



(a) Specimen HOD1

(b) Specimen HOD2

Fig. 16 Development of concrete cracks

outrigger walls. It is noted that quite limit number of cracks developed on the hybrid outrigger arm under the 'protection' from the low-yield steel damper.

Fig. 17 shows the load deflection curves of the Specimen HOD1 under a monotonic load. It was noted that the low-yield steel damper yielded at a applied load near 400 kN as compared with the predicted yielding load for the steel outrigger truss of 570 kN. The displacement recorded at the loading cell was increased continuously until approximately 35 mm after the yield of the steel damper. No apparent un-loading, damage or material degrading was observed on the low-yield damper. In the meantime, maximum strain recorded in the steel section of the bracing member is 1800 micro strain, which is well below the yield strain of the steel member. The strain recorded in the rebar is even lower of 1600 micro strain. This demonstrates the good ductility and energy dispersing potential of the hybrid outrigger system under the protection of the low-yield steel damper.

### 6.2 System test under quasi-static cyclic loads

For Specimen HOD2 tested under quasi-static cyclic

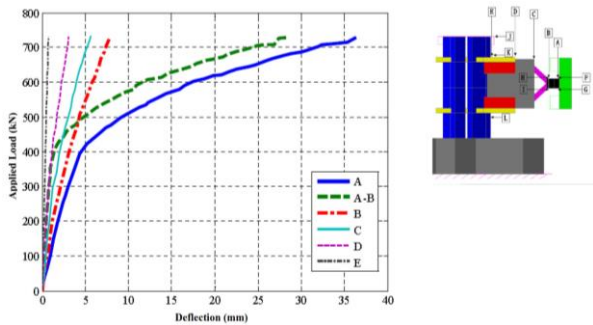


Fig. 17 Load deflection curve for Specimen HOD1

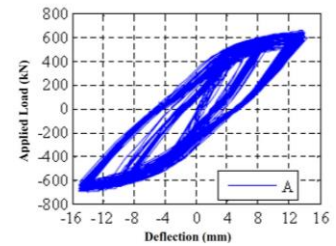
loads, micro concrete cracks occurred near the joint between the outrigger and core walls at a load level 300 kN. Micro cracks of diagonal patterns were observed near the end of outrigger wall at an applied displacement of  $\pm 8$  mm. The overall recorded crack pattern is shown in Fig. 16(b). The low-yield damper started to yield at an applied load level of 400 kN, which is similar to the case of the monotonic test on Specimen HOD1. The maximum crack width recorded is 0.15 mm on the ring beam at the applied displacement of  $\pm 3.5$  mm.

No apparent damage on either the concrete wall or the steel bracing was observed after 30 cycles of  $\pm 13$  mm applied displacement as shown in Fig. 18. While after 58 cycles of maximum applied displacement and loads, debonding was observed at the welded joint between the web and the flange of the low-yield steel damper, and with a 10% degrading in load carrying capacities. The degrading is further developed to be 15% at 60 cycles of the maximum applied displacement before the termination of the test. No yield was observed in either steel bracing members or the rebar in the concrete outrigger and core walls at this extreme applied displacement and large number of cycle. This showed good energy dispersing capacity of such innovative type of outrigger system. The comparison between Fig. 18 for Specimen HOD2 and Fig. 12 for Specimen HOA2 also reveals the effectiveness of the low-yield steel damper towards the enhancement of the energy dispersing capacities of the hybrid outrigger system.

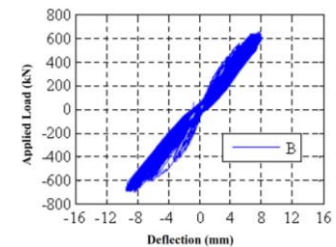
Three-dimensional finite element models were also proposed (Wang 2015) with the incorporation of both geometrical and material non-linearities under monotonic loads. As such, the load-deformation characteristics of the outrigger system at both elastic and large deformation plastic stages can be captured properly. Various structural performance were studied and calibrated including load carrying capacities, load-deformation curves and stress distribution and concentration, etc, which validate the accuracy of the results of test program.

### 7. Conclusions

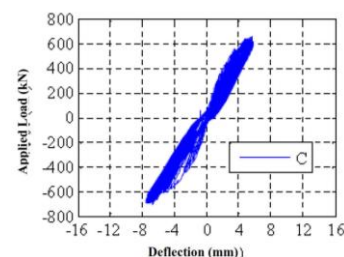
A comprehensive experimental research program was conducted into the structural performance of this new type of hybrid outrigger system. Both the key component and overall system tests were conducted, which reveal the detailed structural response under various levels of applied



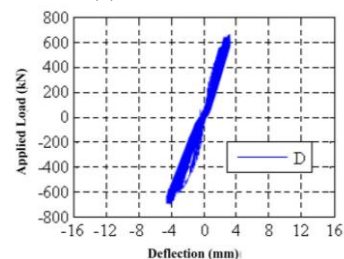
(a) Transmitter A



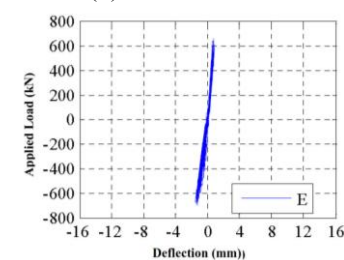
(b) Transmitter B



(c) Transmitter C



(d) Transmitter D



(e) Transmitter E

Fig. 18 Load deflection curve for Specimen HOD2

monotonic and cyclic loads. The following conclusions were reached:

#### Low-yield steel damper

- Both the flange and joint stiffener on the low-yield steel damper are important towards the overall ductility and load carrying capacities of the damper.
- With the thickened flange from 6.7 to 8.3 mm, the ductility of the low-yield steel damper increases greatly as discussed in Section 5. As such, Careful engineering

and detailing are necessary.

#### Hybrid outrigger arm

No apparent damage on hybrid outrigger arm was observed at the 30 cycles of the applied load at the specimen ultimate load capacity under the maximum deflection of  $\pm 15$  mm. While the degrading in both the strength and the stiffness happened when the maximum applied displacement was larger than 20 mm. More severe cracks on concrete outrigger wall were observed through the process, which implies the necessity of the protection from the low-yield steel damper as the sacrificing member.

#### Hybrid outrigger system with damper

- The comparison between Fig. 18 for Specimen HOD2 and Fig. 12 for Specimen HOA2 also reveals the effectiveness of the low-yield steel damper towards the enhancement of the energy dispersing capacities of the hybrid outrigger system.

- No yield was observed in either steel bracing members or the rebar in the concrete outrigger and core walls at the extreme applied cyclic load and displacement and large number of cycles under the 'protection' from the 'fuse' of the low-yield steel damper. This showed good energy dispersing capacity of such new type of hybrid outrigger system.

It was demonstrated that both the steel bracing and concrete outrigger wall are able to work compositely with the low-yield steel damper and exhibits both good load carrying capacities and energy dispersing performance through the test program. The experimental studies provide detailed structural understanding towards such new type of outrigger system. It has the potential to be applied and enhance the overall structural performance of the high-rise structures under extreme levels of loads. More analytical and numerical investigation is to be conducted and calibrated for the establishment of the parametric studies and new design rules of such new hybrid outrigger system.

## References

- ASTM (2011), E2126-11: Standard Test Methods for Cyclic (Reversed) Load Test for Shear Resistance of Vertical Elements of the Lateral Force Resisting Systems for Buildings, ASTM.
- Bayati, Z., Mahdikhani, M. and Rahaei, A. (2008), "Optimized use of multi-outriggers system to stiffen tall buildings", *The 14th World Conference on Earthquake Engineering*, 40-44, Beijing, China.
- China Academy of Building Research (CABR) (1997), Specification of Test Methods for Earthquake Resistant Building, CABR.
- Coull, A. and Lao, W.H.O. (1988), "Outrigger braced structures subjected to equivalent static seismic loading", *Proceedings of 4th International Conference on Tall Buildings*.
- Gholipour, M., Asadi, E. and Alinia, M.M. (2015), "The use of outrigger system in steel plate shear wall structures", *Adv. Struct. Eng.*, **18**(6), 853-872.
- Hoenderkamp, J.C.D. (2004), "Shear wall with outrigger trusses on wall and column foundations", *Struct. Des. Tall Spec. Build.*, **13**(1), 73-87.
- Lee, D. (2016), "Additive 2D and 3D performance ratio analysis for steel outrigger alternative design", *Steel Compos. Struct.*, **20**(5), 1133-1153.
- Lee, D., Shin S., Lee, J. and Lee, K. (2015), "Layout evaluation of building outrigger truss using material topology optimization", *Steel Compos. Struct.*, **19**(2), 263-275.
- Lee, J., Minsik, B. and Kim, J.Y. (2008), "An analytical model for high-rise wall-frame structures with outriggers", *Struct. Des. Tall Spec. Build.*, **17**(4), 839-851.
- Malekinejad, M. and Reza R. (2011), "Free vibration analysis of tall buildings with outrigger-belt truss system", *Earthq. Struct.*, **2**(1), 89-107.
- Moon, K.S. (2013), "Outrigger structures for twisted, tilted and tapered tall buildings", *Structures and Architecture: Concepts, Applications and Challenges-Proceedings of the 2nd International Conference on Structures and Architecture*, ICSA, 77-81.
- Moon, K.S. (2015), "Structural design and construction of complex-shaped tall buildings", *Int. J. Eng. Technol.*, **7**(1), 30-42.
- Moudarres, F.R. and Coull, A. (1985), "Free vibration of outrigger based structures", *Proc. Instit. Civil Eng.*, **79**(1), 105-117.
- Nie, J.G., Ding, R., Fan, J.S. and Tao, M.X. (2014), "Seismic performance of joints between k-style outrigger trusses and concrete cores in tall buildings", *J. Struct. Eng.*, ASCE, **140**(12).
- Nouri, F. and Ashtari, P. (2015), "Weight and topology optimization of outrigger-based tall steel structures subjected to the wind loading using GA", *Wind Struct.*, **20**(4), 134-154.
- Park, H.S., Lee, E., Choi, S.W., Oh, B.K., Cho, T.J. and Kim, Y. (2016), "Genetic-algorithm-based minimum weight design of an outrigger system for high-rise buildings", *Eng. Struct.*, **117**, 496-505.
- Sabrina, F. and Tabassum, F. (2016), "Optimum position of steel outrigger system for high rise composite buildings subjected to wind loads", *Adv. Steel Construct.*, **12**(2), 134-153.
- Smith, B.S. and Irawan, S. (1981), "Parameter study of outrigger-braced tall building structures", *J. Struct. Div.*, **107**(10), 2001-2014.
- Smith, B.S. and Irawan, S. (1983), "Formulae for optimum drift resistance of outrigger braced tall building structures", *Comput. Struct.*, **17**(1), 45-50.
- Tan, P., Fang, C.J., Chang, C.M., Spencer, B.F. and Zhou, F.L. (2015), "Dynamic characteristics and novel energy dissipation systems with damped outrigger", *Eng. Struct.*, **98**, 128-140.
- Wang, A.J. (2010), "A study on composite end-plate connections with flexible tensile reinforcements and shear connectors", *Can. J. Civil Eng.*, **37**, 1437-1450.
- Wang, A.J. (2015), "Re-engineering composite connections for a higher construction and cost effectiveness", *11th International Conference Advances in Steel-Concrete Composite Structures*, Beijing, China, 538-543.
- Wang, A.J. (2011), "Studies on composite joints under gravity and lateral loads", *Aust. J. Struct. Eng.*, **12**, 69-85.
- Wu, J.R. and Li, Q.S. (2003), "Structural performance of multi-outrigger-braced tall buildings", *Struct. Des. Tall Spec. Build.*, **12**(2), 155-176.
- Zhang, J. (2007), "Safety analysis of optimal outriggers location in high-rise building structures", *J. Zhejiang Univ. Sci.*, **8**(2), 264-269.
- Zhou, Y. and Li, H. (2014), "Analysis of high-rise steel structure with viscous damped outrigger", *Struct. Des. Tall Spec. Build.*, **23**(13), 963-979.
- Zhou, Y., Zhang, C. and Lu, X. (2017), "Seismic performance of a damping outrigger system for tall buildings", *Struct. Control Hlth. Monit.*, **24**(1), 135-149.